INFECTION AND IMMUNITY, Dec. 2000, p. 6988–6996 Vol. 68, No. 12
0019-9567/00/$04.00+0

Identification of Discrete Domains within Gonococcal Transferrin-Binding Protein A That Are Necessary for Ligand Binding and Iron Uptake Functions

IAN C. BOULTON,[1]† MARY KATE YOST,[1] JAMES E. ANDERSON,[2] AND CYNTHIA NAU CORNELISSEN[1]*

Department of Microbiology and Immunology, Medical College of Virginia Campus of Virginia Commonwealth University, Richmond, Virginia 23298,[1] and Department of Medicine, School of Medicine, University of North Carolina at Chapel Hill, Chapel Hill, North Carolina 27599[2]

Received 5 June 2000/Returned for modification 11 August 2000/Accepted 29 August 2000

The availability of free iron in vivo is strictly limited, in part by the iron-binding protein transferrin. The pathogenic *Neisseria* spp. can sequester iron from this protein, dependent upon two iron-repressible, transferrin-binding proteins (TbpA and TbpB). TbpA is a TonB-dependent, integral, outer membrane protein that may form a β-barrel exposing multiple surface loops, some of which are likely to contain ligand-binding motifs. In this study we propose a topological model of gonococcal TbpA and then test some of the hypotheses set forth by the model by individually deleting three putative loops (designated loops 4, 5, and 8). Each mutant TbpA could be expressed without toxicity and was surface exposed as assessed by immunoblotting, transferrin binding, and protease accessibility. Deletion of loop 4 or loop 5 abolished transferrin binding to whole cells in solid- and liquid-phase assays, while deletion of loop 8 decreased the affinity of the receptor for transferrin without affecting the copy number. Strains expressing any of the three mutated TbpAs were incapable of growth on transferrin as a sole iron source. These data implicate putative loops 4 and 5 as critical determinants for receptor function and transferrin-iron uptake by gonococcal TbpA. The phenotype of the ΔL8TbpA mutant suggests that high-affinity ligand interaction is required for transferrin-iron internalization.

Neisseria gonorrhoeae is the causative agent of the sexually transmitted disease gonorrhea, which has an annual incidence rate of more than 62 million cases worldwide (53). While frequently asymptomatic, gonococcal infection can be associated with serious sequelae, including salpingitis, endometritis, ectopic pregnancy, and infertility in women (49). In addition, gonococcal disease enhances the human immunodeficiency virus titer in seminal plasma of coinfected men, presumably increasing the likelihood of disease transmission (11). In light of these factors, compounded by increased antibiotic resistance (25) and the lack of an effective vaccine, gonorrhea remains a serious public health problem.

Iron is an essential nutrient for all microorganisms (21); however, free iron is rare in the human body, generally being complexed by a number of high-affinity binding proteins, including transferrin (Tf) in plasma and lactoferrin in secretions and macrophages (9). A total of 100% of clinical isolates of *N. gonorrhoeae* can obtain iron from human Tf (40), while approximately 50% of gonococcal isolates can obtain iron from human lactoferrin (39). The ability to use human proteins as iron sources may allow the gonococcus to overcome bacteriostatic iron limitation, which is typical in vivo (9). In contrast to other bacteria, the Tf-iron uptake system employed by pathogenic neisseriae is siderophore independent (3), relying instead on direct association between a surface-exposed bacterial receptor and ligand (3, 48). The receptor is specific for human Tf (31, 32), and Tf-iron internalization is energy (38) and Ton (5, 14) dependent.

The gonococcal Tf receptor is composed of two iron-regulated, Tf-binding proteins designated TbpA and TbpB (14). TbpA is highly conserved among the pathogenic neisseriae (12) and is a member of the TonB-dependent family of integral outer membrane proteins (16). Consistent with other proteins within this group (27, 34, 44), TbpA is likely to form a TonB-regulated transmembrane β-barrel, through which iron can enter the periplasm. Recent crystallographic analyses of FhuA (35) and FepA (8) have demonstrated the involvement of surface-exposed loops in ligand binding. In addition, these studies demonstrated that FhuA and FepA each have an amino-terminal globular domain, which serves as a "plug" in the interior of the transmembrane pore (35). This domain was found to contain a conserved pentameric sequence referred to as the "TonB box" (46), a region that has been shown to interact with the energy transducer TonB (4, 10, 23, 30, 45). Thus, it is probable that the TonB box of TbpA likewise interacts with the periplasmic protein TonB, thereby energizing the Tf receptor and enabling iron internalization.

TbpB is more variable than TbpA, with molecular masses that range from 78 to 86 kDa in *N. gonorrhoeae* (2, 13) and from 65 to 85 kDa in *N. meningitidis* (33, 43, 47). TbpB is lipidated and exposed on the outer leaflet of the bacterial outer membrane (2, 33). Although both Tbps specifically and independently bind human Tf, TbpB selectively binds the ferrated form of this protein while TbpA binds both ferrated and apo Tf (7, 18).

Efficient utilization of Tf as a sole iron source requires expression of both gonococcal Tbps (2). A gonococcal mutant lacking TbpB exhibited decreased Tf-iron internalization relative to the wild-type strain, suggesting that while TbpB expression increases the efficiency of the receptor, it is not es-

* Corresponding author. Mailing address: Department of Microbiology and Immunology, Medical College of Virginia Campus of Virginia Commonwealth University, Box 980678, Richmond, VA 23298-0678. Phone: (804) 225-4121. Fax: (804) 828-9946. E-mail: cncornel@hsc.vcu.edu.

† Present address: Department of Medical Genetics and Microbiology, University of Toronto, Toronto, Ontario, Canada.

TABLE 1. Strains and plasmids used in this study

Strain or plasmid	Description	Source or reference
E. coli		
DH5αMCR	F$^-$ *mcrA* Δ(*mrr-hsdRMS-mcrBC*) ϕ80Δ*lacZ*ΔM15 Δ(*lacZYA-argF*)U169 *endA1 recA1 deoR thi-1 phoA supE441-gyrA96 relA1*	Gibco-BRL
INVαF′	F′ *endA1 recA1 hsdR17*(r_k^-, m_k^+) *supE44 thi-1 gyrA96 relA1* Φ80*lacZ*ΔM15 Δ(*lacZYA-argF*)U169	Invitrogen
N. gonorrhoeae		
FA19	Wild-type	40
FA6747	TbpA$^-$ [*tbpA*::mTn*3*(cm)]	16
FA6905	TbpB$^-$ (Δ*tbpB*)	18
FA6935	TbpA TonB-box mutant	14
FA6815	TbpA$^-$ TbpB$^-$ (*tbpB*::Ω)	2
MCV201	ΔL*5*TbpA	This study
MCV202	ΔL*5*TbpA TbpB$^-$	This study
MCV203	ΔL*4*TbpA	This study
MCV204	ΔL*4*TbpA TbpB$^-$	This study
MCV205	ΔL*8*TbpA	This study
MCV206	ΔL*8*TbpA TbpB$^-$	This study
Plasmids		
pBSIISK(+)	Amp^r	Stratagene
pET21	Amp^r	Novagen
pCR2.1	Amp^r Kan^r	Invitrogen
pUNCH412	pBSIISK(+) containing *Hin*dIII to *Xba*I fragment encoding TbpA	15
pVCU201	pCR2.1 containing 5′ half of ΔL*5tbpA* (*Hin*dIII-*Bam*HI)	This study
pVCU204	pCR2.1 containing 3′ half of ΔL*5tbpA* (*Bam*HI-*Xho*I)	This study
pVCU205	pET21 containing entire ΔL*5tbpA* (*Hin*dIII-*Xho*I)	This study
pVCU206	pCR2.1 containing 5′ half of ΔL*4tbpA* (*Hin*dIII-*Bam*HI)	This study
pVCU207	pCR2.1 containing 3′ half of ΔL*4tbpA* (*Bam*HI-*Xho*I)	This study
pVCU208	pET21 containing entire ΔL*4tbpA* (*Hin*dIII-*Xho*I)	This study
pVCU209	pCR2.1 containing 5′ half of ΔL*8tbpA* (*Hin*dIII-*Bam*HI)	This study
pVCU210	pCR2.1 containing 3′ half of ΔL*8tbpA* (*Bam*HI-*Xho*I)	This study
pVCU211	pET21 containing entire ΔL*8tbpA* (*Hin*dIII-*Xho*I)	This study

sential for Tf-iron internalization (2). In contrast, expression of TbpA is absolutely required for Tf-iron growth and Tf-iron internalization (16), consistent with its role as a transmembrane pore for Tf bound iron. Cornelissen and Sparling (18) demonstrated that TbpA and TbpB are in close proximity to one another and may interact, at least transiently, on the surface of intact gonococci. Surface exposure and Tf-binding characteristics of the cell-associated TbpA-TbpB complex are dependent upon a wild-type Ton system and TonB-box at the amino terminus of TbpA (14).

In this study, we propose a model of gonococcal TbpA that combines computer analysis with observed sequence conservation among TonB-dependent receptors and sequence diversity among gonococcal TbpA sequences. We suggest that TbpA may form a β-barrel composed of 22 transmembrane strands and probably has a periplasmic globular domain equivalent to that described for FhuA (35) and FepA (8). We have tested aspects of this model by individually deleting three regions of gonococcal TbpA, each predicted to form an extracellular, surface-exposed loop. We assessed the surface exposure and function of these deletion derivatives of TbpA and determined that, while expression of loops 4 and 5 of TbpA was critical for the Tf-binding function of this receptor, expression of loop 8 was required for optimal ligand interaction.

MATERIALS AND METHODS

Bacterial strains, plasmids, and media. The bacterial strains and plasmids used in this study are described in Table 1. Unless otherwise stated, gonococci were grown on plates containing GC medium base (Difco) with Kellogg's supplement I (1%) (26) and 12 μM $Fe(NO_3)_3$ in a 5% CO_2 atmosphere at 35°C. For growth in iron-stressed conditions, gonococci were cultured in liquid CDM medium (51) which was pretreated with Chelex-100 (Bio-Rad) to remove residual iron. CDM-agarose plates containing 2.5 μM Tf (30% iron saturated) were used to assess the ability of gonococcal strains to utilize Tf-bound iron. Plasmids were propagated in *Escherichia coli* strains (Table 1) cultured on Luria-Bertani plates (37) containing appropriate antibiotics (50 μg of ampicillin or kanamycin per ml).

Standard recombinant DNA techniques and DNA sequencing. Isolation of plasmid DNA, digestion with restriction endonucleases and subsequent ligation were carried out according to manufacturer's recommendations. PCR amplification was carried in standard conditions (Gibco-BRL) with annealing temperatures optimized for each set of oligonucleotide primers. DNA was sequenced using a 377 DNA sequencer (Applied Biosystems) at the Virginia Commonwealth University Nucleic Acids Core Facility. The template was supplied as plasmid DNA, purified using the Wizard Mini-Prep system (Promega). Nucleotide positions are numbered in accordance with the gonococcal *tbpA* sequence from strain FA19 deposited in GenBank under the accession no. M96731 (16).

Gonococcal transformation. Mutated *tbpA* genes were transformed into gonococcal strains according to the method described by Gunn and Stein (22). Briefly, piliated gonococci were resuspended in GC broth to a density of approximately 2×10^8 CFU/ml. Approximately 100 CFU were spotted onto GC agar plates, followed immediately by linearized plasmid preparations, which had been purified using the Wizard DNA clean-up kit (Promega). Following overnight growth, individual colonies were subcultured and then screened for the incorporation *tbpA* mutations into the chromosome. This analysis involved subjecting colony lysates to PCR using oligonucleotide primers designed to amplify a diagnostic product. Single colonies were passaged, and the genotype was confirmed by DNA sequencing.

Solid-phase binding assays. Whole-cell binding analyses were carried out using gonococci grown in iron-deficient, liquid CDM media as described above. After 3 h of iron-limited growth, normalized amounts of culture were applied to nitrocellulose filters. Blots were probed with horseradish peroxidase (HRP)-Tf (1 μg/ml) as described previously (6) and were developed with Opti-4-CN (Bio-Rad) according to manufacturer's recommendations. Duplicate blots were probed using an anti-TbpA polyclonal serum raised against recombinant meningococcal TbpA from strain SD (1), which cross-reacts with gonococcal TbpA. This sera was preabsorbed against whole, iron-stressed gonococcal strain FA6747 (Table 1) to remove nonspecific, cross-reacting antibodies against antigens other than TbpA. Dot blots were subsequently probed with a goat anti-rabbit immu-

noglobulin G (IgG)-HRP conjugate and developed with Opti-4-CN (Bio-Rad) according to the manufacturer's recommendations.

Liquid-phase Tf-binding assay. Liquid-phase Tf-binding assays were performed essentially as previously described (18). In these assays, iron-stressed gonococci were mixed with various amounts of iodinated, iron-saturated Tf in the presence or absence of unlabeled competitor Tf (iron saturated). After 20 min, the unbound, iodinated Tf was removed by filtration through 0.45-μm-pore-size nitrocellulose (Millipore Multi-Screen microtiter dish MAHV N45). The amount of bound Tf was quantitated with a gamma scintillation counter. The binding assays were standardized to whole-cell protein by performing protein assays (bicinchoninic acid assay; Pierce) on iron-stressed cultures. Three identical experiments, including growth and iron stress, were carried out; the datum points represent the mean of three independent experiments. Specific binding was calculated by subtracting nonspecific binding (detected in the presence of excess competitor) from total counts for each Tf concentration. The specific activity of the iodinated Tf was 1.61×10^6 cpm/μg. Copy number and K_d estimates were obtained using Lundon software (Lundon Software) (36).

Protease-accessibility assay. Protease accessibility experiments were performed as previously described (18). Briefly, iron-stressed whole gonococci (grown in CDM) were treated with trypsin (Sigma-Aldrich) at concentrations of 0.5 to 2.5 μg/ml for 0 to 30 min. Proteolysis was stopped by addition of 0.6 trypsin-inhibiting units of aprotinin (Sigma-Aldrich), and whole-cell lysates were prepared from samples taken at 10-min intervals. In some experiments, ferrated Tf was added prior to protease exposure, to a final concentration of 100 nM. Whole-cell proteins were resolved by sodium dodecyl-sulfate polyacrylamide gel electrophoresis (SDS-PAGE) using 7.5% acrylamide gels (29). Western blots were probed with anti-TbpA polyclonal rabbit sera or with HRP-Tf (to detect TbpB) according to previously described methods (18).

Immunofluorescence microscopy. Immunofluorescence microscopy was used to confirm the surface exposure of TbpA on intact gonococci. Iron-stressed, whole cells from gonococcal strains FA19 (positive control), FA6747 (negative control), and MCV201 (Table 1) were mixed with dilutions anti-TbpA polyclonal rabbit sera (raised against meningococcal TbpA from strain SD) (1) in the presence of immunoglobulin-free bovine serum albumin (Sigma-Aldrich) as a blocking reagent. Preimmune rabbit sera were also used as a negative control. Unbound antibody was removed by centrifugation, and cells were then applied to glass microscope slides and fixed by immersion in 100% methanol. These slides were probed with goat anti-rabbit IgG conjugated to fluorescein isothiocyanate (Sigma-Aldrich), and cells were counterstained with Eriochrome Black (Integrated Diagnostics). Samples were visualized using an Olympus BHA microscope equipped with a BH2RFL reflected fluorescence attachment and a PM-10AD photomicrographic system (Olympus Corp).

RESULTS

Development of a topology model of gonococcal TbpA and selection of loops for deletion analysis. We initially used the method of Klebba et al. (28) to convert the TbpA sequence into a two-dimensional topology model. We identified potential amphipathic β-strands with the algorithm MOMENT (19) and putative β-turns with the algorithm βTURNPRED (52). In addition, our original model located most stretches of hydrophilic residues and all six cysteine residues within predicted surface-exposed loops. We modified this computer-generated model by superimposing on it observed sequence variation among TbpAs from the pathogenic neisseriae, *Haemophilus influenzae*, *Actinobacillus pleuropneumoniae*, *Pasteurella haemolytica*, and *Moraxella catarrhalis* (12). We reasoned that sequence diversity would be enriched in surface-exposed regions that were accessible to immune pressure and that conserved domains would be either inaccessible or functionally constrained. Figure 1 represents the latest version of our TbpA topology model and encompasses a further modification based upon pairwise comparisons between TbpA and the recently crystallized TonB-dependent receptor, FepA (8). Since the coordinates of all FepA residues have been elucidated in the crystal structure, we created a pairwise alignment between gonococcal TbpA and FepA and used this alignment to identify putative β-strand endpoints. With this alignment, we also identified an amino-terminal, 162-residue domain of TbpA that was 29% identical and 44% similar to the analogous region of FepA. This amino-terminal region was shown in the FepA crystal structure to form an essentially globular "plug" that occludes the lumen of the β-barrel (8). We have depicted the homologous region of TbpA (residues 1 to 162) in a similar position in Fig. 1. This region is very well conserved among the neisserial TbpAs (12), consistent with the suggestion that this domain is inaccessible from the outside and therefore not subject to immune pressure.

We generated a series of antipeptide sera against surface-exposed loops predicted from our TbpA topology model (12). One of these sera, directed against a portion of loop 5, reacted with wild-type, surface-exposed TbpA (12). This observation suggested that loop 5 was surface exposed, and thus we focused initial deletion efforts on this loop. We chose to delete putative loop 4 because it was situated next to loop 5 but, in contrast to loop 5, was relatively well conserved in sequence among the pathogenic neisseriae (12). We chose loop 8 for deletion analysis because it was divergent among the neisseriae and was therefore likely to be surface exposed.

Construction of ΔL4TbpA, ΔL5TbpA, and ΔL8TbpA mutants. The method for the construction of TbpA-encoding plasmids from which loop 4 was deleted is schematically represented in Fig. 2. To delete loop 4 from TbpA of strain FA19 (Table 1), we used the oligonucleotide pair HIND and oVCU-16 to amplify the 5′ half of *tbpA*; to amplify the 3′ half of *tbpA*, we used oVCU-17 and oVCU-7 (Table 2 and Fig. 2). These oligonucleotides introduced novel *Bam*HI sites flanking the sequence that encodes loop 4. The separate PCR fragments were cloned independently into pCR2.1, yielding pVCU206 and pVCU207 (Table 1 and Fig. 2). Subsequently, the 5′ and 3′ halves of *tbpA* were excised and cloned into the pET21 expression vector in a single three-part ligation, producing plasmid pVCU208 (Table 1 and Fig. 2). Sequence analysis confirmed the deletion of 144 bp of gonococcal *tbpA* in this plasmid. The deleted region encoded 48 amino acids, which were replaced by two residues: glycine and serine. However, two additional single-base mutations were noted in the mutated *tbpA*. The first was a silent mutation, and the second exchanged an alanine for a glycine. Given the conservative nature of these base changes, no corrective mutagenesis was undertaken.

Construction and characterization of Δ*L5tbpA* and Δ*L8tbpA* were carried out essentially as described above, substituting oligonucleotides oVCU-16 and oVCU-17 with oLBAM and oUBAM (Table 2), respectively, in the construction of Δ*L5tbpA* and substituting oligonucleotides oVCU-16 and oVCU-17 with oligonucleotides oVCU-25 and oVCU-24 (Table 2), respectively, in the construction of Δ*L8tbpA* (Table 1). The 5′ and 3′ halves of Δ*L5tbpA* were cloned into pCR2.1, producing plasmids pVCU201 and pVCU204 (Table 1). Combining the inserts from these clones in pET21 generated plasmid pVCU205 (Table 1). Sequence analysis confirmed a deletion of 174 bp within an otherwise-unaltered *tbpA* gene and established that the 58 residues comprising loop 5 were replaced by a single proline. The 5′ and 3′ halves of Δ*L8tbpA* were cloned into pCR2.1, producing plasmids pVCU209 and pVCU210 (Table 1), respectively. Combining the inserts from these plasmids in pET21 generated pVCU211 (Table 1). Sequence analysis of this plasmid confirmed the deletion of 69 bp corresponding to 23 amino acids. This region was replaced by two residues (glycine and serine), while the remaining TbpA sequence was unaltered.

Following construction in *E. coli*, the plasmids encoding ΔL4TbpA, ΔL5TbpA, and ΔL8TbpA were individually transformed into gonococcal strains FA19 (wild type) and FA6905 ($TbpB^-$), resulting in strains MCV201 through MCV206 (Table 1). Following transformation, the regions surrounding each deletion were PCR amplified from mutant chromosomes, the products were sequenced, and no additional nucleotide

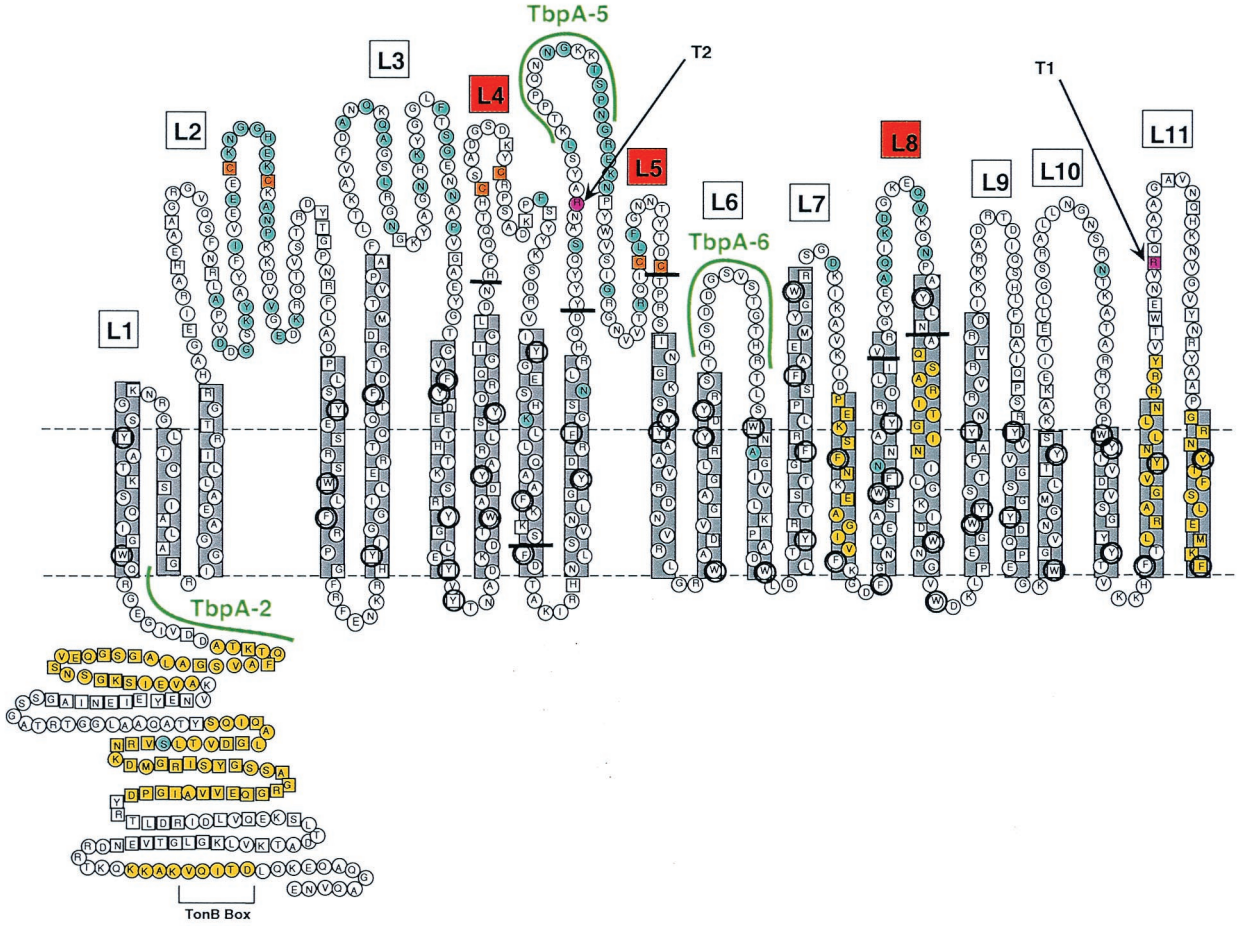

FIG. 1. Putative topology model of gonococcal TbpA. Horizontal dotted lines represent the planes of the gonococcal outer membrane. The predicted amphipathic β-strands (22 in total) are shown in gray boxes. Putative surface exposed loops are numbered L1 to L11. Loops 4, 5, and 8 are indicated by red boxes, and the endpoints of the ΔL4, ΔL5, and ΔL8 deletions are indicated by short horizontal black bars. Residues that are conserved among all 17 TbpAs sequenced to date (12) are indicated by the squares. Residues that fall within previously characterized TonB homology domains (16) are shaded yellow. Residues that are variant among a panel of 5 gonococcal TbpAs (12) are shaded blue. Aromatic residues are circled. Cysteine residues are shaded orange. Two predicted trypsin cleavage sites are shaded pink. Although the TbpA sequence contains many other predicted trypsin cleavage sites, cleavage at these two sites would generate proteolytic cleavage products that most closely match the observed sizes of trypsin digest products T1 and T2 (see text). The sequences of three peptides used to generate antipeptide antibodies (12) are highlighted in green.

changes were noted. This confirmed the successful incorporation of the mutant *tbpA* genes into the wild-type gonococcal chromosome.

Solid-phase Tf binding by gonococcal TbpA deletion mutants. To determine the functionality of the TbpA loop-deletion mutants, we first tested the ability of strains expressing deleted TbpAs to bind Tf in a solid-phase binding assay. As shown in Fig. 3A, strains expressing TbpA loop deletions and a functional TbpB (MCV201, MCV203, and MCV205) retained Tf-binding capability as expected. In the absence of a functional TbpB, strains MCV202 (ΔL5TbpA, TbpB$^-$) and MCV204 (ΔL4TbpA, TbpB$^-$) were no longer competent for Tf binding unlike their isogenic parent FA6905, which expresses a full-length TbpA (Fig. 3A). MCV206 (ΔL8TbpA, TbpB$^-$) bound somewhat less Tf than did the wild-type strain in the same assay (Fig. 3A), suggesting that this strain, while capable of Tf binding, did so with diminished affinity or capacity. Thus, deletion of either loop 4 or loop 5 prevented ligand binding by TbpA and indicated that these regions contain residues that are directly or indirectly required for Tf binding. The apparent reduction of Tf binding to ΔL8TbpA suggested that the presence loop 8 could be important for high-affinity interactions between TbpA and its ligand.

Localization of gonococcal TbpA deletion mutants. The inability of the loop 4 and loop 5 deletion mutants to bind Tf in the solid-phase assay could have been the result of inappropriate processing or localization of the mutant proteins. To address this possibility, duplicate whole-cell dot blots were probed with a polyclonal anti-TbpA serum that recognized surface-exposed TbpA. As shown in Fig. 3B, this serum bound to all strains expressing either wild-type TbpA (FA19 and FA6905) or mutated TbpAs (strains MCV201 to MCV206). Strains FA6747 and FA6815 (both TbpA$^-$) were not recognized by this serum (Fig. 3B). These observations indicated that wild-type TbpA and ΔL4TbpA, ΔL5TbpA, and ΔL8TbpA were each surface exposed and accessible to antibody under these conditions.

Since cell lysis could effect the apparent exposure of TbpA and its deletion derivatives, we sought to confirm the dot blot result of ΔL5TbpA using immunofluorescence microscopy, in which the integrity of the reactive organisms could be assessed by counterstain. As in the dot blot experiment, anti-TbpA serum bound to whole, iron-stressed gonococci expressing ΔL5TbpA, not to the isogenic *tbpA* mutant FA6747 (data not shown). These results confirmed the results of the dot blot (Fig. 3B), which indicated that this deleted version of TbpA

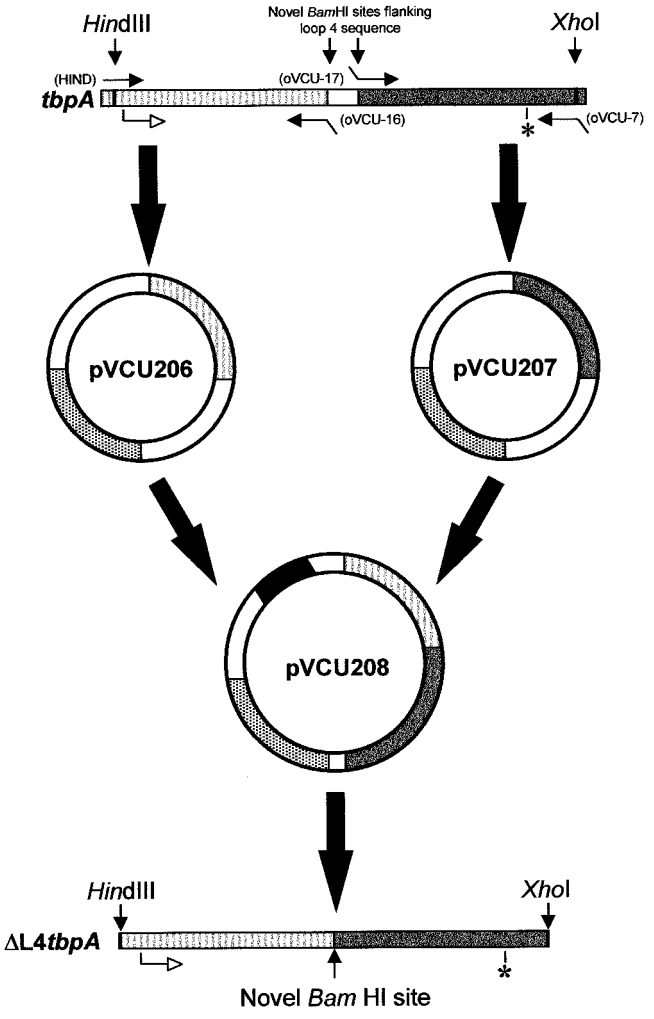

FIG. 2. Construction of ΔL4TbpA. The 5′ (striped) and 3′ (gray) PCR-amplified halves of *tbpA* were individually cloned into pCR2.1, which contains a gene encoding ampicillin resistance (stippled bar). This procedure resulted in plasmids pVCU206 and pVCU207, respectively. These inserts were excised and ligated together in pET21 producing pVCU208, which contained Δ*L4tbpA*, downstream of a T7 promoter (black bar). The position of the TbpA start codon is shown as an open arrow, and that of the TbpA stop codon is marked with an asterisk. Approximate positions of oligonucleotides are indicated by closed arrows, with their respective names indicated in parentheses.

was surface exposed in iron-stressed gonococci, as was the wild-type protein.

Liquid-phase Tf binding by gonococcal TbpA deletion mutants. We used a liquid-phase Tf-binding assay to quantitate the binding phenomena associated with the TbpA deletion derivatives in the solid-phase binding assay. The curves shown in Fig. 4 represent the amount of specific Tf bound as a function of Tf concentration, which ranged from 1.2 to 160 nM. As in the solid-phase Tf binding assay, neither MCV204 (ΔL4TbpA, TbpB$^-$) nor MCV202 (ΔL5TbpA, TbpB$^-$) bound any detectable Tf in this assay. In contrast, MCV206 (ΔL8TbpA, TbpB$^-$) bound Tf with nearly the same capacity as the wild-type strain but with a much lower affinity. Whereas the wild-type TbpA (expressed by FA6905 in the absence of TbpB) bound Tf with a K_d of approximately 2.8 nM (Fig. 4 and reference 18), the ΔL8TbpA mutant bound Tf with a K_d of 22 nM. The capacity of the wild-type and ΔL8TbpA mutant strain were virtually indistinguishable, with copy numbers of 8.2×10^8 and 8.3×10^8 receptors/μg of total cell protein, respectively. These data confirmed and extended the results of the solid-phase Tf binding analysis, indicating that deletion of loop 4 or loop 5 prevented ligand binding completely, whereas deletion of loop 8 resulted in a 10-fold decrease in the affinity of TbpA for Tf without affecting the copy number.

Growth of TbpA deletion mutants with transferrin as a sole iron source. To assess the impact of TbpA mutagenesis on Tf-iron utilization, strains MCV201 to MCV206 were plated on minimal medium containing partially saturated Tf as the sole iron source. As shown previously, the presence of TbpB increases the efficiency of Tf-iron uptake but is not required for growth on Tf as a sole iron source (2). All of the TbpA deletion derivatives failed to grow on Tf, regardless of the presence of a functional TbpB (Fig. 5), indicating that deletion of putative loop 4 or 5 rendered TbpA unable to bind Tf and, despite apparent surface exposure, unable to facilitate the uptake of iron from Tf. Interestingly, ΔL8TbpA, which bound Tf with lower affinity but equal capacity, did not facilitate iron internalization. All strains grew equally well on GC base medium supplemented with $Fe(NO_3)_3$.

Protease accessibility of TbpA in deletion mutants. We previously identified energy-dependent conformational changes in the Tf receptor based partly on the results of limited proteolysis of whole, iron-stressed gonococci (14). Thus, we used trypsin accessibility of the TbpA deletion derivatives as a measure of wild-type surface exposure and overall conformation. When wild-type TbpA was exposed to low concentrations of trypsin, two diagnostic products were generated, one with a molecular mass of 95.2 kDa (T1) and the other with a molecular mass of 54.9 kDa (T2) (Fig. 6A and reference 18). A mutant TbpA lacking a functional TonB box (14) likewise demonstrated a trypsin accessibility pattern characterized by wild-type-sized T1 and T2 products (Fig. 6A). The deletion derivatives of TbpA were universally accessible to exogenous trypsin, a finding consistent with normal processing and surface exposure of these proteins. The proteolytic fragments generated by trypsin digestion of the deletion derivatives did not differ greatly in size from those generated by cleavage of the wild-type protein, with T1 and T2 equivalents apparent in two out of the three deletion mutants (Fig. 6A). The sizes of T1 and T2 equivalents in these mutants were consistent with the number of amino acids that had been deleted in each construct. In addition to T1 and T2, ΔL4TbpA spontaneously proteolyzed, producing a detectable breakdown product at 0 min of trypsin exposure (Fig. 6A). This slight instability could have resulted from deletion of most of a proposed membrane-spanning β-strand (see Fig. 1) in this construct.

Trypsin digestion of ΔL5TbpA yielded a T1 equivalent but

TABLE 2. Oligonucleotides used in this study

Name	Oligonucleotide sequence[a]	Amplification product
oVCU-16	5′-**GGATCC**GTTGTCCAAACCGATGCCCT-3′	ΔL4TbpA
oVCU-17	5′-**GGATCC**TTCGATACCGG^{2}CAAAATCCG-3′	ΔL4TbpA
oUBAM	5′-A**GGATCC**CACGCCGCGCAGCATCAA-3′	ΔL5TbpA
oLBAM	5′-A**GGATCC**TGATGGCGGAGATTAGAGC-3′	ΔL5TbpA
oVCU-24	5′-**GGATCC**AATCAAATCGCGGTAGGCATT-3′	ΔL8TbpA
oVCU-25	5′-**GGATCC**GCCCAAAGCGCGCGGATT-3′	ΔL8TbpA
oVCU-7	5′-**CTCGAG**GCTCTAGAAACCCCAACGCAG-3′	All
HIND	5′-CGAAGAGTTGGGGCGGATGGTT-3′	All

[a] Mismatched bases, corresponding to mutagenic restriction sites, are shown in boldface. The superscript "2" indicates an error incorporated into the oligonucleotide.

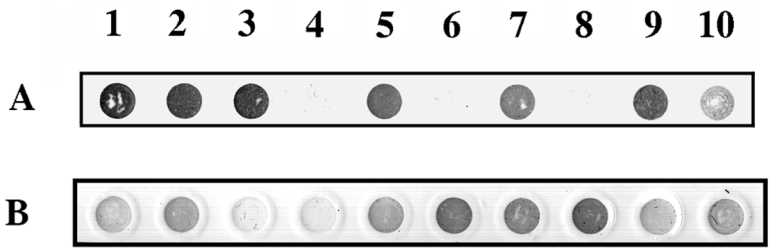

FIG. 3. Whole-cell, solid-phase Tf-binding assay. Whole, iron-stressed gonococci were spotted onto nitrocellulose filters and probed with HRP-Tf (A) or anti-TbpA polyclonal serum (B). Numbering refers to the following gonococcal strains; 1, FA19 (wild type); 2, FA6905 (TbpA$^+$ TbpB$^-$); 3, FA6747 (TbpA$^-$ TbpB$^+$); 4, FA6815 (TbpA$^-$ TbpB$^-$); 5, MCV201 (ΔL5TbpA, TbpB$^+$); 6, MCV202 (ΔL5TbpA, TbpB$^-$); 7, MCV203 (ΔL4TbpA, TbpB$^+$); 8, MCV204 (ΔL4TbpA, TbpB$^-$); 9, MCV205 (ΔL8TbpA, TbpB$^+$); and 10, MCV 206 (ΔL8TbpA, TbpB$^-$). Images were scanned using a Hewlett-Packard ScanJet 6300c. Final images were annotated using Adobe Photoshop 4.0.

no T2 equivalent. This was not surprising since the size of the T2 product generated from the wild-type TbpA was consistent with cleavage of an accessible trypsin site within putative loop 5 (T2 in Fig. 1), which had been deleted in this construct. To confirm the mapping of this endpoint, we probed the wild-type trypsin T2 cleavage product (data not shown) with a series of antipeptide sera that have been previously described (12). The T2 proteolytic product generated by wild-type TbpA digestion was reactive in a Western blot with antiserum generated against peptide TbpA-2 (Fig. 1) but was not reactive with sera generated against peptides TbpA-5 and TbpA-6 (Fig. 1). Cumulatively, these results indicated that the T2 product generated from wild-type TbpA contained the TbpA-2 peptide sequence but not the TbpA-5 or TbpA-6 peptide sequences (Fig. 1), therefore locating the carboxy-terminal endpoint of T2 between TbpA-2 and TbpA-5. In contrast to ΔL5TbpA, limited proteolysis of ΔL8TbpA generated a T1 equivalent that was smaller than the wild-type T1, consistent with the deletion of loop 8, and a T2 equivalent that was identical in size to the wild-type T2. These observations are consistent with our proposed model in which the two accessible trypsin sites fall on either side of putative loop 8.

Protease accessibility of TbpA in the presence of transferrin. We have previously demonstrated that TbpA to which Tf is bound is less accessible to exogenously added trypsin than unliganded TbpA (18), while a de-energized, TonB-box mutant of TbpA was almost completely inaccessible to trypsin in the presence of ligand (14). As shown in Fig. 6B, the proteolytic digestion patterns of ΔL4TbpA and ΔL5TbpA were unchanged in the presence of Tf, whereas proteolysis of ΔL8TbpA was inhibited in the presence of Tf, similar to wild-type TbpA. These observations are consistent with our assertion that neither ΔL4TbpA nor ΔL5TbpA bound Tf because the presence of ligand did not effect the extent of proteolysis. In contrast, since trypsin accessibility was inhibited by ligand addition to ΔL8TbpA, we conclude that this derivative retained Tf binding capabilities, an idea consistent with the results of Tf-binding assays (Fig. 3 and 4).

Protease accessibility of TbpB in gonococcal deletion mutants. Previously, we demonstrated that TbpB is protected from limited proteolysis only in the presence of an energized TbpA (14). Thus, we analyzed the accessibility of TbpB to trypsin in presence of the TbpA deletion derivatives to access

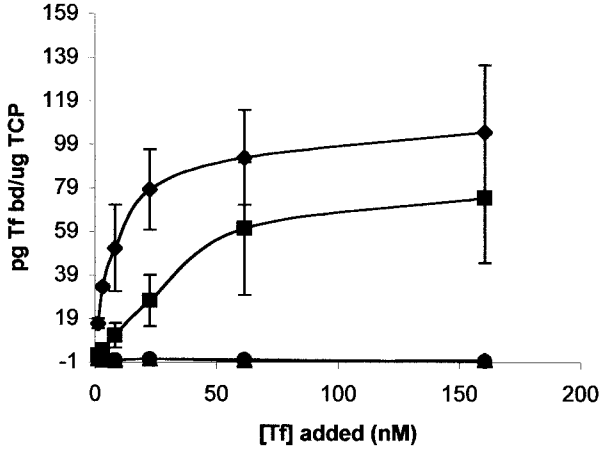

FIG. 4. Equilibrium-phase Tf binding by TbpA deletion mutants. The plot shows the amount of specifically bound Tf (in picograms bound per microgram of total cell protein [TCP]) as a function of Tf concentration. ◆, Binding to FA6905 (TbpA$^+$ TbpB$^-$); ■, binding to MCV206 (ΔL8TbpA, TbpB$^-$); ▲, binding to MCV202 (ΔL5TbpA, TbpB$^-$); ●, binding to MCV204 (ΔL4TbpA, TbpB$^-$). The datum points are the means of three independent experiments. Error bars indicate the standard deviations within each triplicate set.

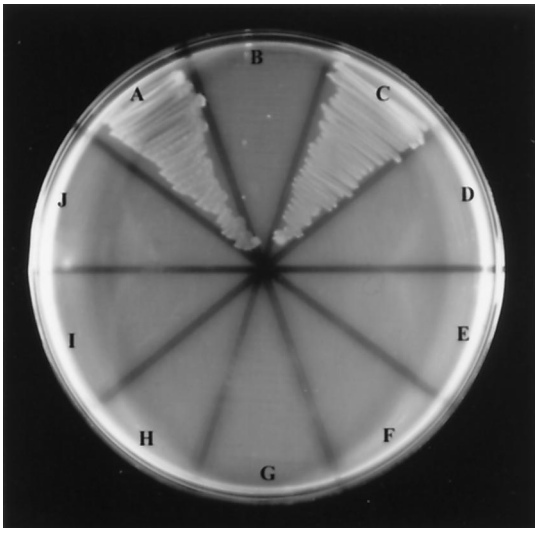

FIG. 5. Growth of gonococcal strains using Tf as a sole iron source. Gonococcal strains were grown on CDM-agarose plates, supplemented with Tf (30% iron saturated) as an iron source. Sector labeling refers to the following gonococcal strains: A, FA19 (wild type); B, FA6747 (TbpA$^-$ TbpB$^+$); C, FA6905 (TbpA$^+$ TbpB$^-$); D, FA6815 (TbpA$^-$ TbpB$^-$); E, MCV201 (ΔL5TbpA, TbpB$^+$); F, MCV202 (ΔL5TbpA, TbpB$^-$); G, MCV203 (ΔL4TbpA, TbpB$^+$); H, MCV204 (ΔL4TbpA, TbpB$^-$); I, MCV205 (ΔL8TbpA, TbpB$^+$); and J, MCV 206 (ΔL8TbpA, TbpB$^-$). Images were scanned using a Hewlett-Packard ScanJet 6300c. The final images were annotated using Adobe Photoshop 4.0.

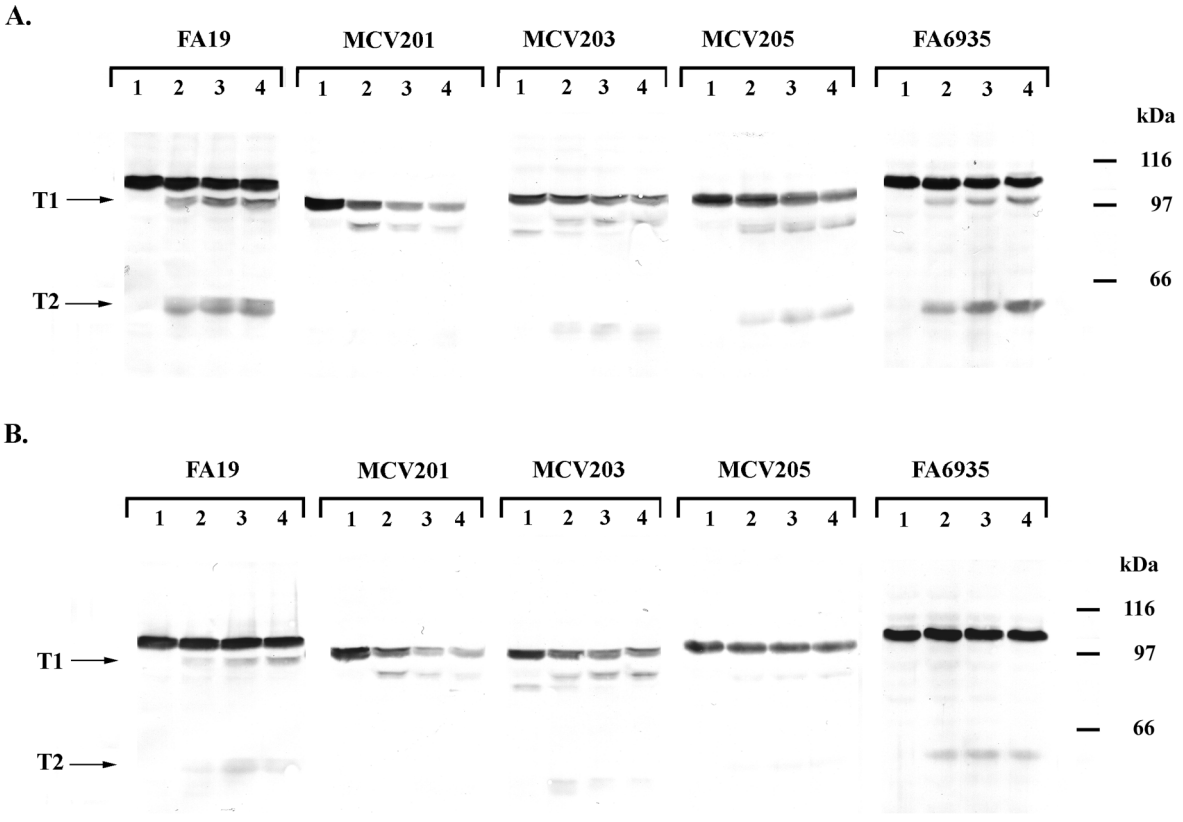

FIG. 6. Trypsin accessibility of mutant TbpAs in the presence and absence of ligand. (A) Whole, iron-stressed cells from the indicated gonococcal strains were treated with trypsin (0.5 μg/ml) for 0 min (lane 1), 10 min (lane 2), 20 min (lane 3), or 30 min (lane 4) as indicated above each panel. Whole-cell lysates were prepared from the trypsinized cells, and the proteins were separated by SDS-PAGE. The resulting Western blots were probed with polyclonal anti-TbpA serum (16). (B) Whole, iron-stressed cells from the indicated gonococcal strains were exposed to 100 nM iron-saturated Tf and then treated with trypsin (0.5 μg/ml) for 0 min (lane 1), 10 min (lane 2), 20 min (lane 3), or 30 min (lane 4) as indicated above each panel. The resulting Western blots were probed with polyclonal anti-TbpA serum (16). The labels T1 and T2 on the left of each panel indicate the positions of two characteristic products that resulted from limited proteolysis of TbpA. Approximate positions of molecular mass standards are indicated in kilodaltons on the right of each panel. Images were scanned using a Hewlett-Packard ScanJet 6300c. The final images were annotated using Adobe Photoshop 4.0.

their ability to interact with and functionally protect TbpB from trypsin. When coexpressed with ΔL4TbpA, ΔL5TbpA, or ΔL8TbpA TbpB was protected at levels equivalent to those observed with wild-type TbpA (data not shown), indicating that the mutant TbpAs could interact with TbpB such that a portion of the TbpB population was resistant to trypsin, similar to the situation seen with the wild-type TbpA.

DISCUSSION

In this study, we propose a topological model of gonococcal TbpA in which this protein forms an outer membrane pore composed of 22 transmembrane β-strands. In addition, we suggest that gonococcal TbpA has a periplasmic globular domain, one similar to that identified in the crystal structures of two other TonB-dependent receptors, FepA (8) and FhuA (35). The authors of those studies hypothesized that the globular domain serves as a "plug" (35) or "hatch" (8) that occludes the lumen of the β-barrel formed by other transmembrane β-strands. Given the extent of conservation between TbpA and the TonB-dependent receptors and also the relative lack of divergence among neisserial TbpA sequences in this region (12), we suggest that this domain may have a similar location and function in gonococcal TbpA. The large size, structural complexity, and dynamic nature of both TbpA (14) and Tf (50), suggest that multiple surface-exposed epitopes may determine the ligand-binding characteristics of this receptor. Thus, our proposed topological model includes 11 putative loops, any or all of which could include ligand-binding domains.

In the current study, we determined the phenotypes of mutant gonococcal strains expressing TbpAs deleted of putative loop 4, 5, or 8. These mutant proteins were expressed from the gonococcal chromosome without apparent toxicity or inhibition of bacterial growth. Using solid- and liquid-phase Tf-binding assays, immunoblots, protease accessibility, and TbpB interaction, we confirmed the outer membrane localization of each mutant protein. Extreme structural perturbation of outer membrane proteins typically results in aberrant localization, spontaneous proteolysis and, in some cases, inviability (41, 42). In the absence of these effects, we conclude that the native conformation adopted by wild-type TbpA was broadly conserved among the mutants characterized in this study. The sole exception to this overall conclusion is ΔL4TbpA, which exhibited slight proteolytic instability and therefore native folding might have been effected by deletion of most of proposed β-strand 8 in addition to loop 4. However, as evaluated by the trypsin accessibility pattern of TbpA expressed by this mutant, a large portion of the deleted protein was exported to the surface in a conformation similar to that of wild-type TbpA. The ΔL5TbpA protein was apparently surface exposed and resulted in no spontaneous breakdown products, suggesting

that deletion of this putative loop did not negatively impact protein export. Likewise, the observation of nearly identical numbers of ΔL8TbpA receptors relative to the wild-type receptor in whole-cell, liquid-phase Tf-binding assays indicates that deletion of these loops had no discernible deleterious effects on protein export or surface exposure. Therefore, we suggest that the alteration in Tf binding by these mutants resulted from the deletion of functionally significant epitopes rather than from gross conformational disruption or reduced surface exposure.

Deletion of loop 4 or loop 5 resulted in mutant versions of TbpA that were incapable of Tf binding and that did not support growth on Tf-bound iron, suggesting that these putative loops are critical for ligand interaction and subsequent iron internalization. Even in the presence of a functional TbpB, iron utilization was prevented by deletion of loop 4 or loop 5 from TbpA, indicating that the mere proximity of ferrated Tf (bound to TbpB) was insufficient to allow iron uptake. Deletion of loop 8 from TbpA resulted in a mutant that was capable of binding Tf with a 10-fold decreased affinity relative to wild-type TbpA. However, this deletion mutant was rendered completely incompetent for Tf-iron internalization. These observations suggest that intimate, high-affinity interactions between TbpA and Tf are required for iron removal and subsequent iron transport through the outer membrane.

Limited proteolysis has been used to identify flexible domains in globular enzymes (24) and as a probe of conformational change in soluble proteins (20). In this study, we used accessibility to exogenous protease as a measure of surface exposure and overall membrane topology in the TbpA deletion derivatives. We have previously shown that exposure of surface-exposed TbpA to low concentrations of trypsin produced two diagnostic proteolytic products (18). Although mature TbpA contains 129 predicted trypsin cleavage sites, only two are readily accessible in the membrane-bound, surface-exposed protein. Since protease accessibility is correlated with unstructured, highly flexible, hinge regions (24), we suggest that the trypsin cleavage sites in TbpA might reflect structurally important features of the receptor. The measured size of the largest wild-type proteolytic digestion product (T1) most closely corresponds to a peptide that spans from the mature amino terminus to Arg857, located in putative loop 11. The size of the T2 proteolytic product corresponds in size to a peptide that spans from the mature amino terminus to Arg498, located in putative loop 5. Thus, these regions are predicted to be sufficiently flexible to allow protease cleavage, and might represent hinge regions separating structurally constrained domains.

When we applied the protease susceptibility analysis to the deletion derivatives of TbpA, similarly sized proteolytic products were generated, indicating that the gross topological features of the mutant TbpAs were similar to those expressed by the wild-type strain. Both T1 and T2 equivalents produced by trypsin cleavage of ΔL4TbpA were proportionally smaller than their wild-type counterparts, which is consistent with deletion of loop 4. Only a T1 equivalent was generated by trypsin digestion of ΔL5TbpA, which is consistent with the concomitant deletion of the accessible trypsin site (Arg498) in loop 5. Of the two proteolytic digestion products generated from ΔL8TbpA, the T1 equivalent was proportionally smaller by the size of the loop 8 deletion, but the T2 product was wild-type sized. From this analysis, we conclude that putative loop 8 is located between the two accessible trypsin sites that generated T1 and T2.

We have previously shown that by binding Tf prior to trypsin treatment, the accessibility of TbpA to the protease is inhibited (14, 18). In mutants in which TbpA is de-energized by Ton system defects, TbpA is almost completely protected from proteolysis, suggesting that TonB-derived energy is required for Tf release from the receptor (14). We analyzed the loop deletion mutants for their trypsin accessibility following ligand binding and found that, unlike a de-energized TbpA, all were accessible to trypsin. However, ΔL8TbpA was protected by the presence of ligand to an extent similar to that in wild-type TbpA, a finding consistent with the Tf-binding capabilities of this mutant. Unlike ΔL8TbpA, mutants ΔL4TbpA and ΔL5TbpA were equally susceptible to trypsin cleavage in the presence or absence of ligand, a result consistent with their complete inability to bind Tf.

In a similar analysis, we found that TbpB was protected from exogenous trypsin when coexpressed with either wild-type (14, 18) or mutant TbpA. Using this protease-resistant characteristic of TbpB, we developed a model of energy-dependent, conformational change or complex formation between TbpA and TbpB (14). Because the deletion mutants described in this study protect coexpressed TbpB from trypsin in a manner similar to that seen with wild-type TbpA, we conclude that on whole, iron-stressed gonococci, TbpA and TbpB formed a transient, energy-dependent complex similar to that detected in the wild-type strain. This implies that, under these conditions, the deleted regions were not essential for the preservation of physical proximity between TbpA and TbpB or for their proposed energy-dependent interaction.

Since expression of the Tf receptor is required to initiate infection in a human challenge model of gonococcal infection (17), identification of domains of TbpA that are necessary for the optimal function of this receptor could lead to therapies or prevention strategies aimed at abrogating its function. Thus, loops 4 and 5, which are essential for optimal ligand binding, could constitute novel targets for immunoprophylaxis against gonococcal disease. Alternatively, inhibitors of transferrin binding by these loops might serve as a mode of therapy against an already established infection. Loop 8, which appears to play a more subtle role in Tf binding but nevertheless critically impacts Tf-iron utilization, may also warrant assessment as a candidate vaccine antigen or target of inhibition. We are currently constructing smaller deletions and point mutations to further characterize the complex ligand binding and interactive properties of gonococcal TbpA.

ACKNOWLEDGMENTS

This research was funded by Public Health Service grant AI39523 from the National Institute of Allergy and Infectious Diseases.

We gratefully acknowledge Andrew R. Gorringe for providing polyclonal anti-TbpA polyclonal rabbit serum raised against recombinant meningococcal TbpA and Phillip E. Klebba for his advice in the construction of the TbpA topology model.

REFERENCES

1. **Ala'Aldeen, D. A. A., P. Stevenson, E. Griffiths, A. R. Gorringe, L. I. Irons, A. Robinson, S. Hyde, and S. P. Borriello.** 1994. Immune responses in humans and animals to meningococcal transferrin-binding proteins: implications for vaccine design. Infect. Immun. **62:**2984–2990.
2. **Anderson, J. E., P. F. Sparling, and C. N. Cornelissen.** 1994. Gonococcal transferrin-binding protein 2 facilitates but is not essential for transferrin utilization. J. Bacteriol. **176:**3162–3170.
3. **Archibald, F. S., and I. W. DeVoe.** 1980. Iron acquisition by *Neisseria meningitidis in vitro*. Infect. Immun. **27:**322–334.
4. **Bell, P. E., C. D. Nau, J. T. Brown, J. Konisky, and R. J. Kadner.** 1990. Genetic suppression demonstrates interaction of TonB protein with outer membrane transport proteins in *Escherichia coli*. J. Bacteriol. **172:**3826–3829.
5. **Biswas, G. D., J. E. Anderson, and P. F. Sparling.** 1997. Cloning and functional characterization of *Neisseria gonorrhoeae tonB*, *exbB*, and *exbD* genes. Mol. Microbiol. **24:**169–179.
6. **Blanton, K. J., G. D. Biswas, J. Tsai, J. Adams, D. W. Dyer, S. M. Davis,**

G. G. Koch, P. K. Sen, and P. F. Sparling. 1990. Genetic evidence that *Neisseria gonorrhoeae* produces specific receptors for transferrin and lactoferrin. J. Bacteriol. **172:**5225–5235.
7. **Boulton, I. C., A. R. Gorringe, N. Allison, A. Robinson, B. Gorinsky, C. L. Joannou, and R. W. Evans.** 1998. Transferrin-binding protein B isolated from *Neisseria meningitidis* discriminates between apo and diferric human transferrin. Biochem. J. **334:**269–273.
8. **Buchanan, S. K., B. S. Smith, L. Venkatramani, D. Xia, L. Esser, M. Palnitkar, R. Chakraborty, D. van der Helm, and J. Deisenhofer.** 1999. Crystal structure of the outer membrane active transporter FepA from *Escherichia coli*. Nat. Struct. Biol. **6:**56–63.
9. **Bullen, J. J., H. J. Rogers, and E. Griffiths.** 1978. Role of iron in bacterial infection. Curr. Top. Microbiol. Immunol. **80:**1–35.
10. **Cadieux, N., and R. J. Kadner.** 1999. Site-directed disulfide bonding reveals an interaction site between energy-coupling protein TonB and BtuB, the outer membrane cobalamin transporter. Proc. Natl. Acad. Sci. USA **96:** 10673–10678.
11. **Cohen, M. S., I. F. Hoffman, R. A. Royce, P. Kazembe, J. R. Dyer, C. C. Daly, D. Zimba, P. L. Vernazza, M. Maida, S. A. Fiscus, J. J. Eron, and A. M. R. Group.** 1997. Reduction of concentration of HIV-1 in semen after treatment of urethritis: implications for prevention of sexual transmission of HIV-1. Lancet **349:**1868–1873.
12. **Cornelissen, C. N., J. E. Anderson, I. C. Boulton, and P. F. Sparling.** 2000. Antigenic and sequence diversity in gonococcal transferrin-binding protein A (TbpA). Infect. Immun. **68:**4725–4735.
13. **Cornelissen, C. N., J. E. Anderson, and P. F. Sparling.** 1997. Characterization of the diversity and the transferrin-binding domain of gonococcal transferrin-binding protein 2. Infect. Immun. **65:**822–828.
14. **Cornelissen, C. N., J. E. Anderson, and P. F. Sparling.** 1997. Energy-dependent changes in the gonococcal transferrin receptor. Mol. Microbiol. **26:**25–35.
15. **Cornelissen, C. N., G. D. Biswas, and P. F. Sparling.** 1993. Expression of gonococcal transferrin-binding protein 1 causes *Escherichia coli* to bind human transferrin. J. Bacteriol. **175:**2448–2450.
16. **Cornelissen, C. N., G. D. Biswas, J. Tsai, D. K. Paruchuri, S. A. Thompson, and P. F. Sparling.** 1992. Gonococcal transferrin-binding protein 1 is required for transferrin utilization and is homologous to TonB-dependent outer membrane receptors. J. Bacteriol. **174:**5788–5797.
17. **Cornelissen, C. N., M. Kelley, M. M. Hobbs, J. E. Anderson, J. G. Cannon, M. S. Cohen, and P. F. Sparling.** 1998. The transferrin receptor expressed by gonococcal strain FA1090 is required for the experimental infection of human male volunteers. Mol. Microbiol. **27:**611–616.
18. **Cornelissen, C. N., and P. F. Sparling.** 1996. Binding and surface exposure characteristics of the gonococcal transferrin receptor are dependent on both transferrin-binding proteins. J. Bacteriol. **178:**1437–1444.
19. **Eisenberg, D., M. Schwarz, M. Komaromy, and R. Wall.** 1984. Analysis of membrane and surface protein sequences with the hydrophobic moment plot. J. Mol. Biol. **179:**125–142.
20. **Fontana, A., M. Zambonin, P. P. de Laureto, V. de Filippis, A. Clementi, and E. Scaramella.** 1997. Probing the conformational state of apomyoglobin by limited proteolysis. J. Mol. Biol. **266:**223–230.
21. **Griffiths, E.** 1987. Iron and infection: molecular, physiological and clinical aspects, p. 69–137. *In* J. J. Bullen and E. Griffiths (ed.), The iron-uptake systems of pathogenic bacteria. John Wiley & Sons, Ltd., Chichester, United Kingdom.
22. **Gunn, J. S., and D. C. Stein.** 1996. Use of a non-selective transformation technique to construct a multiply restriction/modification-deficient mutant of *Neisseria gonorhoeae*. Mol. Gen. Genet. **251:**509–517.
23. **Heller, K. J., R. J. Kadner, and K. Gunther.** 1988. Suppression of the *btuB451* mutation by mutations in the *tonB* gene suggests a direct interaction between TonB and TonB-dependent receptor proteins in the outer membrane of *Escherichia coli*. Gene **64:**147–153.
24. **Hubbard, S. J., F. Eisenmenger, and J. M. Thornton.** 1994. Modeling studies of the change in conformation required for cleavage of limited proteolytic sites. Protein Sci. **3:**757–768.
25. **Ison, C. A., J.-A. R. Dillon, and J. W. Tapsall.** 1998. The epidemiology of global antibiotic resistance among *Neisseria gonorrhoeae* and *Haemophilus ducreyi*. Lancet **351:**8–11.
26. **Kellogg, D. S., Jr., W. L. Peacock, Jr., W. E. Deacon, L. Brown, and C. I. Pirkle.** 1963. *Neisseria gonorrhoeae*. I. Virulence genetically linked to clonal variation. J. Bacteriol. **85:**1274–1279.
27. **Killmann, H., R. Benz, and V. Braun.** 1996. Properties of the FhuA channel in the *Escherichia coli* outer membrane after deletion of FhuA portions within and outside the predicted gating loop. J. Bacteriol. **178:**6913–6920.
28. **Klebba, P. E., J. M. Rutz, J. Liu, and C. K. Murphy.** 1993. Mechanisms of TonB-catalyzed iron transport through the enteric bacterial cell envelope. J. Bioenerg. Biomembr. **25:**603–611.
29. **Laemmli, U. K.** 1970. Cleavage of structural proteins during the assembly of the head of bacteriophage T4. Nature **227:**680–685.
30. **Larsen, R. A., D. Foster-Hartnett, M. A. McIntosh, and K. Postle.** 1997. Regions of *Escherichia coli* TonB and FepA proteins essential for in vivo physical interactions. J. Bacteriol. **179:**3213–3221.
31. **Lee, B. C., and L. E. Bryan.** 1989. Identification and comparative analysis of the lactoferrin and transferrin receptors among clinical isolates of gonococci. J. Med. Microbiol. **28:**199–204.
32. **Lee, B. C., and A. B. Schryvers.** 1988. Specificity of the lactoferrin and transferrin receptors in *Neisseria gonorrhoeae*. Mol. Microbiol. **2:**827–829.
33. **Legrain, M., V. Mazarin, S. W. Irwin, B. Bouchon, M.-J. Quentin-Millet, E. Jacobs, and A. B. Schryvers.** 1993. Cloning and characterization of *Neisseria meningitidis* genes encoding the transferrin-binding proteins Tbp1 and Tbp2. Gene **130:**73–80.
34. **Liu, J., J. M. Rutz, J. B. Feix, and P. E. Klebba.** 1993. Permeability properties of a large gated channel within the ferric enterobactin receptor, FepA. Proc. Natl. Acad. Sci. USA **90:**10653–10657.
35. **Locher, K. P., B. Rees, R. Koebnik, A. Mitschler, L. Moulinier, J. P. Rosenbusch, and D. Moras.** 1998. Transmembrane signaling across the ligand-gated FhuA receptor: Crystal structures of free and ferrichrome-bound states reveal allosteric changes. Cell **95:**771–778.
36. **Lundeen, J. E., and J. H. Gordon.** 1986. Computer analysis of binding data, p. 31–49. *In* R. A. O'Brian (ed.), Receptor Binding in Drug Research. Marcel Dekker, New York, N.Y.
37. **Maniatis, T., E. F. Fritsch, and J. Sambrook.** 1982. Molecular cloning: a laboratory manual. Cold Spring Harbor Laboratory, Cold Spring Harbor, N.Y.
38. **McKenna, W. R., P. A. Mickelsen, P. F. Sparling, and D. W. Dyer.** 1988. Iron uptake from lactoferrin and transferrin by *Neisseria gonorrhoeae*. Infect. Immun. **56:**785–791.
39. **Mickelsen, P. A., E. Blackman, and P. F. Sparling.** 1982. Ability of *Neisseria gonorrhoeae*, *Neisseria meningitidis*, and commensal *Neisseria* species to obtain iron from lactoferrin. Infect. Immun. **35:**915–920.
40. **Mickelsen, P. A., and P. F. Sparling.** 1981. Ability of *Neisseria gonorrhoeae*, *Neisseria meningitidis*, and commensal *Neisseria* species to obtain iron from transferrin and iron compounds. Infect. Immun. **33:**555–564.
41. **Newton, S. M. C., J. S. Allen, Z. Cao, Z. Qi, X. Jiang, C. Sprencel, J. D. Igo, S. B. Foster, M. A. Payne, and P. E. Klebba.** 1997. Double mutagenesis of a positive charge cluster in the ligand-binding site of the ferric enterobactin receptor, FepA. Proc. Natl. Acad. Sci. USA **94:**4560–4565.
42. **Newton, S. M. C., J. D. Igo, D. C. Scott, and P. E. Klebba.** 1999. Effect of loop deletions on the binding and transport of ferric enterobactin by FepA. Mol. Microbiol. **32:**1153–1165.
43. **Rokbi, B., V. Mazarin, G. Maitre-Wilmotte, and M.-J. Quentin-Millet.** 1993. Identification of two major families of transferrin receptors among *Neisseria meningitidis* strains based on antigenic and genomic features. FEMS Microbiol. Lett. **110:**51–58.
44. **Rutz, J. M., J. Liu, J. A. Lyons, J. Goranson, S. K. Armstrong, M. A. McIntosh, J. B. Feix, and P. E. Klebba.** 1992. Formation of a gated channel by a ligand-specific transport protein in the bacterial outer membrane. Science **258:**471–475.
45. **Schoffler, H., and V. Braun.** 1989. Transport across the outer membrane of *Escherichia coli* K12 via the FhuA receptor is regulated by the TonB protein of the cytoplasmic membrane. Mol. Gen. Genet. **217:**378–383.
46. **Schramm, E., J. Mende, V. Braun, and R. M. Kamp.** 1987. Nucleotide sequence of the colicin B activity gene *cba*: consensus peptapeptide among TonB-dependent colicins and receptors. J. Bacteriol. **169:**3350–3357.
47. **Schryvers, A. B., and B. C. Lee.** 1989. Comparative analysis of the transferrin and lactoferrin binding proteins in the family *Neisseriaceae*. Can. J. Microbiol. **35:**409–415.
48. **Simonson, C., D. Brener, and I. W. DeVoe.** 1982. Expression of a high-affinity mechanism for acquisition of transferrin iron by *Neisseria meningitidis*. Infect. Immun. **36:**107–113.
49. **Swasdio, K., S. Rugpao, T. Tansathit, C. Uttavichai, P. Jongusuk, T. Vutayavanich, A. Oranratanachai, N. Pruthitada, S. Peerakom, W. Ittipunkul, P. J. Rowe, and M. E. Ward.** 1996. The association of *Chlamydia trachomatis*/gonococcal infection and tubal factor infertility. J. Obstet. Gynaecol. Res. **22:**331–340.
50. **Ward, J. H.** 1987. The structure, function, and regulation of transferrin receptors. Investig. Radiol. **22:**74–83.
51. **West, S. E. H., and P. F. Sparling.** 1987. Aerobactin utilization by *Neisseria gonorrhoeae* and cloning of a genomic DNA fragment that complements *Escherichia coli fhuB* mutations. J. Bacteriol. **169:**3414–3421.
52. **Wilmot, C. M., and J. M. Thornton.** 1990. Beta-turns and their distortions: a proposed new nomenclature. Protein Eng. **3:**479–493.
53. **World Health Organization.** 1996. Sexually transmitted disease fact sheet. World Health Organization, Geneva, Switzerland.

Editor: D. L. Burns